

# Nanocrystalline materials for hydrogen storage

M. JURCZYK

*Institute of Materials Science and Engineering, Poznan University of Technology,  
Skłodowska-Curie 5 Sq., 60-965 Poznan, Poland*

Hydrogen storage materials research is entered a new and exciting period with the advent of the nanocrystalline alloys. This presentation reviews research at the Poznan University of Technology, on the synthesis and properties of nanocrystalline hydride electrode materials. In our work, nanocrystalline materials have been synthesized by mechanical alloying (MA) followed by annealing. Examples of the materials include TiFe-, ZrV<sub>2</sub>-, LaNi<sub>5</sub>- and Mg<sub>2</sub>Ni-type phases. The properties of hydrogen host materials can be modified substantially by alloying to obtain the desired storage characteristics. The hydrogen storage properties of nanocrystalline ZrV<sub>2</sub>- and LaNi<sub>5</sub>-type powders prepared by mechanical alloying and annealing show no big difference with those of melt casting (microcrystalline) alloys. Finally, the electronic properties of nanocrystalline alloys will be presented. The synthesized alloys were used as negative electrode materials for Ni-MH battery.

(Received January 18, 2006; accepted March 23, 2006)

*Keywords:* Nanocrystalline materials, Hydrogen absorbing materials, Ni-MH batteries

## 1. Introduction

During the last years, the mechanical alloying (MA) process has been successfully used to prepare a variety of alloy powders including powders exhibiting supersaturated solid solutions, quasicrystals, amorphous phases and nano-intermetallic compounds [1]. During MA process, the powder particles are periodically trapped between colliding balls and are plastically deformed. Such a feature occurs by the generation of a wide number of dislocations as well as other lattice defects. Furthermore, the ball collisions cause fracturing and cold welding of the elementary particles, forming clean interfaces at the atomic scale. Further milling leads to an increase in the interface number and the sizes of the elementary component area decrease from millimeter to submicrometer lengths. Concurrently to this decrease of the elementary distribution, some nanocrystalline intermediate phases are produced inside the particles.

Recently, MA has been used to make nanocrystalline TiFe, LaNi<sub>5</sub>, ZrV<sub>2</sub> and Mg<sub>2</sub>Ni type alloys [2-5]. The nanostructured materials show substantially enhanced absorption and desorption kinetics, even at relatively low temperatures [6].

TiFe and ZrV<sub>2</sub> alloys crystallize in the cubic CsCl and MgCu<sub>2</sub> structures and at room temperature they absorb up to 2 H/f.u. and 5.5 H/f.u., respectively. On the other hand, LaNi<sub>5</sub> alloy crystallizes in the hexagonal CaCu<sub>5</sub> structure and at room temperature can absorb up to 6 H/f.u. Nevertheless, the application of these types of materials in batteries has been limited due to slow absorption/desorption kinetics in addition to a complicated activation procedure. The properties of hydrogen host materials can be modified substantially by alloying to

obtain the desired storage characteristics, e.g. proper capacity at a favourable hydrogen pressure [7]. TiFe alloy is lighter and cheaper than the LaNi<sub>5</sub>-type material. To improve the activation of this alloy several approaches have been adopted. For example, the replacement of Fe by some amount of transition metals to form secondary phase may improve the activation properties of TiFe. On the other hand, the electrochemical activity of ZrV<sub>2</sub>-type materials can be stimulated by substitution, in which Zr is partially replaced by Ti and V is partially replaced by other transition metals (Cr, Mn and Ni). Independently, it was found that the respective replacement of La and Ni in LaNi<sub>5</sub> by small amounts of Zr and Al resulted in a prominent increase in the cycle life time without causing much decrease in capacity [8].

Magnesium-based alloys have been extensively studied during last years, as well [9]. The polycrystalline Mg<sub>2</sub>Ni alloy can reversibly absorb and desorb hydrogen only at high temperatures. Upon hydrogenation at 523 K, Mg<sub>2</sub>Ni transforms into the hydride phase Mg<sub>2</sub>NiH<sub>4</sub>. Substantial improvements in the hydriding-dehydriding properties of Mg<sub>2</sub>Ni metal hydrides could be possibly achieved by the formation of nanocrystalline structures [6]. The hydrogen content in Mg<sub>2</sub>NiH<sub>4</sub> is also relatively high, being 3.6 wt%, whereas only 1.5 wt% in LaNi<sub>5</sub>H<sub>6</sub>.

The main objective of the present paper is to review the advantages of some nanomaterials, their application in batteries and the challenges involved in their fabrication. In this work, the electrochemical properties of TiFe-, ZrV<sub>2</sub>-, LaNi<sub>5</sub>- and Mg<sub>2</sub>Ni-type alloys are investigated. Details of the processing used and the enhancement of properties due to the nanoscale structures are presented. The measurements of the properties are also included. Then the effect of the nickel and graphite coating on the structure of some alloys and

electrodes characteristics is studied. Finally, the electronic properties of nanocrystalline alloys with electrochemical behaviour of sealed Ni-MH batteries using nanocrystalline TiFe-type anodes are given.

## 2. Experimental

Conventionally the materials were prepared by arc melting of stoichiometric amounts of the constituent elements (purity 99.8% or better) in an argon atmosphere. The alloy lump was pulverized in few hydriding/dehydriding cycles to a fine powder ( $\leq 45 \mu\text{m}$ ).

Another processing method, mechanical alloying was performed under argon atmosphere using a SPEX 8000 Mixer Mill. The purity of the starting materials was at least 99.8 % and the composition of the starting powder mixture corresponded to the stoichiometry of the „ideal” reactions. The as-milled powders were heat treated at 723–1073 K for 0.5 h under high purity argon to form ordered phases (see text for details). The powders were characterized by means of X-ray diffraction (XRD) using a Co  $K\alpha$  radiation, at the various stages during milling, prior to annealing and after annealing. The crystallite sizes were estimated by Scherrer method as well by atomic force microscopy (AFM) method.

The MA and annealed powders were mixed and milled for 1 h or 30 min with 10 wt.% nickel powder (3–7  $\mu\text{m}$ , 99.9 %) or graphite powder (45  $\mu\text{m}$ , 99.999 %) in a SPEX Mixer Mill, respectively. The weight ratio of hard steel balls to mixed powder was 30:1. The mechanically alloyed materials, in nanocrystalline forms, with 10 wt% addition of Ni powder, were subjected to electrochemical measurements as working electrodes. A detailed description of the electrochemical measurements was given in Refs. [4,5].

## 3. Results and discussion

The effect of MA processing was studied by X-ray diffraction, microstructural investigations as well as by electrochemical measurements. In the present study, TiFe-,  $\text{ZrV}_2$ -,  $\text{LaNi}_5$ - and  $\text{Mg}_2\text{Ni}$ -type alloys have been prepared by mechanical alloying (Fig. 1). Formation of these alloys was achieved by annealing the amorphous materials in high purity argon atmosphere (Table 1).

### 3.1 TiFe-type materials

Fig. 2 shows a series of XRD spectra of mechanically alloyed Ti-Fe powder mixture (53.85 wt% Ti + 46.15 wt% Fe) subjected to milling at increasing time. The originally sharp diffraction lines of Ti and Fe gradually become broader (Fig. 2b) and their intensity decreases with milling time. The powder mixture milled for more than 20 h has transformed completely to the amorphous phase, without formation of other phase (Fig. 2c). During the MA process the crystalline size of the Ti decreases with mechanical alloying time and reaches a steady value of 20 nm after

15 h of milling. This size of crystallites seems to be favourable to the formation of an amorphous phase, which develops at the Ti-Fe interfaces. Formation of the nanocrystalline alloy TiFe was achieved by annealing the amorphous material in high purity argon atmosphere at 973 K for 0.5 h (Table 1). All diffraction peaks were assigned to those of CsCl-type structure with cell parameter  $a = 0.2973 \text{ nm}$ . When nickel is added to  $\text{TiFe}_{1-x}\text{Ni}_x$  the lattice constant  $a$  increases.

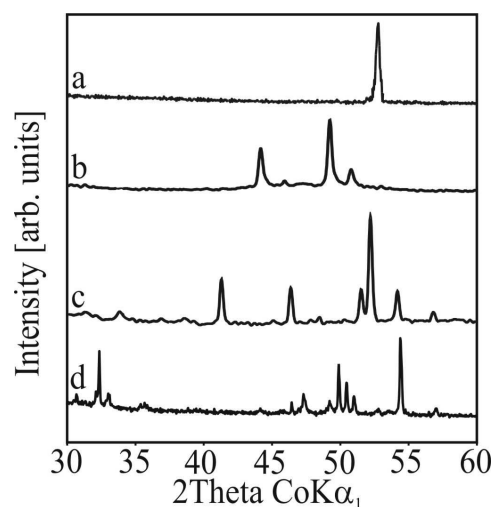


Fig. 1. XRD spectra of nanocrystalline TiFe (a),  $\text{ZrV}_2$  (b),  $\text{LaNi}_5$  (c) and  $\text{Mg}_2\text{Ni}$  (d) alloys produced by mechanical alloying followed by annealing (TiFe MA for 20 h and heat treated at 973 K for 0.5 h;  $\text{ZrV}_2$  MA for 40 h and heat treated at 1073 K for 0.5 h;  $\text{LaNi}_5$  MA 30 h and heat treated at 973 K for 0.5 h;  $\text{Mg}_2\text{Ni}$  MA 90 h and heat treated at 723 K for 0.5 h).

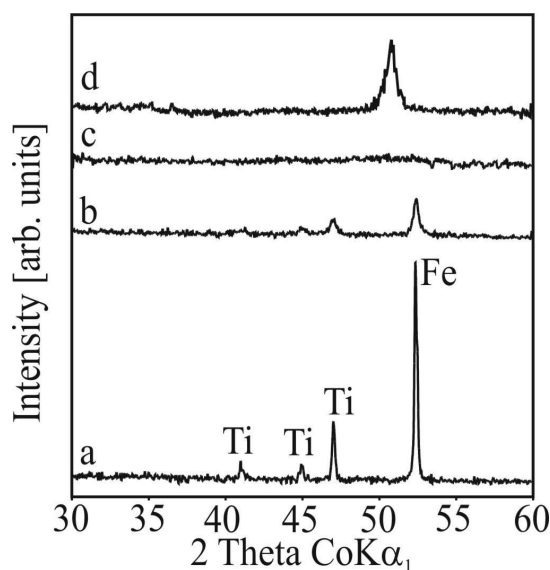


Fig. 2. XRD spectra of a mixture of Ti and Fe powders MA for different times in argon atmosphere: a) initial state (elemental powder mixture), b) after MA for 2 h, c) after MA for 20 h and d) heat treated at 973 K for 0.5 h.

Table 1. Properties of studied nanocrystalline alloys.

Alloy composition	MA time [h]	Heat treatment [K/h]	Structure	Lattice constants		d [nm]	Discharge capacity at 3 <sup>rd</sup> cycle [mAh g <sup>-1</sup> ]
				a [nm]	c [nm]		
TiFe	20	973/0.5	CsCl	0.2973	–	20	7.50 *
TiFe <sub>0.25</sub> Ni <sub>0.75</sub>	20	973/0.5	CsCl	0.3010	–	–	155 **
ZrV <sub>2</sub>	25	1073/0.5	MgCu <sub>2</sub>	0.750	–	35	0 *
Zr <sub>0.35</sub> Ti <sub>0.65</sub> V <sub>0.85</sub> Cr <sub>0.26</sub> Ni <sub>1.30</sub>	30	1073/0.5	MgZn <sub>2</sub>	0.4921	0.8011	–	260 **
LaNi <sub>5</sub>	30	973/0.5	CaCu <sub>5</sub>	0.5012	0.3975	25	90 **
LaNi <sub>3.75</sub> Mn <sub>0.75</sub> Al <sub>0.25</sub> Co <sub>0.25</sub>	30	973/0.5	CaCu <sub>5</sub>	0.5075	0.4039	–	255 **
Mg <sub>2</sub> Ni	90	723/1	Mg <sub>2</sub> Ni	0.5216	1.3246	30	100 *
Mg <sub>1.5</sub> Mn <sub>0.5</sub> Ni	90	723/1	Ti <sub>2</sub> Ni	1.1321	–	–	241 *

d – crystallite size

\* – current density of charging and discharging was 4 mA g<sup>-1</sup>

\*\* – current density of charging and discharging was 40 mA g<sup>-1</sup>

The electrochemical pressure-composition (e.p.c.) isotherms for absorption and desorption of hydrogen were obtained from the equilibrium potential values of the electrodes, measured during intermittent charge and/or discharge cycles at constant current density [10]. Due to the amorphous nature of the studied alloys prior to annealing, the hydrogen absorption-desorption characteristics are not satisfactory. Compared with nanocrystalline TiFe its storage capacity was considerably smaller. Annealing causes transformation from the amorphous to the crystalline structure and produces grain boundaries. Anani et al. noted that grain boundaries are necessary for the migration of the hydrogen into the alloy [2]. It is worth noting, that the characteristics for polycrystalline and nanocrystalline materials are very similar in respect to hydrogen contents, but there are small differences in the plateau pressures. The hydrogenation behaviour of the amorphous structure was different than that of the thermodynamically stable, crystalline material. For amorphous TiFe material the plateau totally disappears. When the amount of Ni in TiFe<sub>1-x</sub>Ni<sub>x</sub> was increased, the pressure in the plateau region continued to decrease and the hydrogen storage capacity was increased.

The discharge capacity of electrodes prepared from TiFe alloy powder by application of MA and annealing displayed a very low capacity (7.50 mA h g<sup>-1</sup> at 4 mA g<sup>-1</sup> discharge current) whereas the arc melted ones have none [10]. The reduction of the powder size and the creation of new surfaces is effective for the improvement of the hydrogen absorption rate.

Materials obtained when Ni was substituted for Fe in TiFe lead to great improvement in activation behaviour of the electrodes. It was found that the increasing nickel content in TiFe<sub>1-x</sub>Ni<sub>x</sub> alloys leads initially to an increase in discharge capacity, giving a maximum at x = 0.75 [11]. In the annealed nanocrystalline TiFe<sub>0.25</sub>Ni<sub>0.75</sub> powder, discharge capacity of up to 155 mA h g<sup>-1</sup> (at 40 mA g<sup>-1</sup> discharge current) was measured. The electrodes mechanically alloyed and annealed from the elemental powders displayed the maximum capacities at around the 3-rd cycle but, especially for x = 0.5 and 0.75 in TiFe<sub>1-x</sub>Ni<sub>x</sub> alloy, degraded slightly with cycling. This may

be due to the easy formation of the oxide layer (TiO<sub>2</sub>) during the cycling.

On the other hand, the discharge capacity of nanocrystalline TiNi<sub>0.6</sub>Fe<sub>0.1</sub>Mo<sub>0.1</sub>Cr<sub>0.1</sub>Co<sub>0.1</sub> powder has not changed much during cycling. The alloying elements Mo, Cr and Co, substituted simultaneously for iron atoms in nanocrystalline Ti(Fe-Ni) master alloy have prevented oxidation of this electrode material.

### 3.2 ZrV<sub>2</sub>-type alloys

The nanocrystalline ZrV<sub>2</sub> and Zr<sub>0.35</sub>Ti<sub>0.65</sub>V<sub>0.85</sub>Cr<sub>0.26</sub>Ni<sub>1.30</sub> alloys were synthesized by mechanical alloying followed by annealing. The electrochemical properties of nanocrystalline powders were measured and compared with those of amorphous material. The behaviour of MA process has been studied by X-ray diffraction. The powder mixture milled for more than 25 h has transformed absolutely to the amorphous phase. Formation of ordered alloys was achieved by annealing the amorphous materials in high purity argon atmosphere at 1073 K for 0.5 h (Fig. 1b).

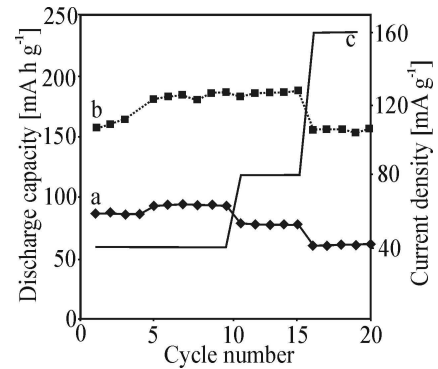


Fig. 3. Discharge capacity as a function of cycle numbers of electrode prepared with (a) amorphous and (b) nanocrystalline Zr<sub>0.35</sub>Ti<sub>0.65</sub>V<sub>0.85</sub>Cr<sub>0.26</sub>Ni<sub>1.30</sub> (solution, 6M KOH; temperature, 293 K). The charge conditions were: 40 mA g<sup>-1</sup>; The discharge conditions were plotted on Figure (c); cut-off potential vs. Hg/HgO/6M KOH was of -0.7 V.

Fig. 3 shows the discharge capacities of the amorphous and nanocrystalline electrodes as a function of charge/discharge cycling number. The electrode prepared with nanocrystalline  $Zr_{0.35}Ti_{0.65}V_{0.85}Cr_{0.26}Ni_{1.30}$  material showed better activation and higher discharge capacities. This improvement is due to a well-established diffusion path for hydrogen atoms along the numerous grain boundaries. The electrochemical results show very little difference between the nanocrystalline and polycrystalline powders, as compared with the substantial difference between these and the amorphous powder. In the annealed nanocrystalline  $Zr_{0.35}Ti_{0.65}V_{0.85}Cr_{0.26}Ni_{1.30}$  powders prepared by mechanical alloying and annealing discharge capacities up to  $150 \text{ mA h g}^{-1}$  (at  $160 \text{ mA g}^{-1}$  discharge current) have been measured.

It has been shown, that the electrochemical properties of hydrogen storage alloys, which do not contain nickel, can be stimulated by high-energy ball-milling of the precursor alloys with a small amount of nickel powders [12]. The  $ZrV_2$  and  $Zr_{0.5}Ti_{0.5}V_{0.8}Mn_{0.8}Cr_{0.4}$  alloy powders have been prepared using HEBM of precursor alloys with nickel powder. It was confirmed that discharge capacity of electrodes prepared with application of  $ZrV_2$  and  $Zr_{0.5}Ti_{0.5}V_{0.8}Mn_{0.8}Cr_{0.4}$  alloy powders with 10 wt% of nickel powder addition was impossible to estimate because of extremely high polarization. In the electrodes prepared with application of high-energy ball-milled  $ZrV_2/Ni$  and  $Zr_{0.5}Ti_{0.5}V_{0.8}Mn_{0.8}Cr_{0.4}/Ni$  alloy powders with 10 wt% of nickel powder the discharge capacities were considerably improved, and they increased from 0 to  $110 \text{ mA h g}^{-1}$  and  $214 \text{ mA h g}^{-1}$ , respectively.

The alloy elements such as Ti substituted for Zr and Mn, Cr substituted for V in  $ZrV_2/Ni$ -based materials greatly improved the activation behaviour of the electrodes. It is worth noting that annealed nanocrystalline  $ZrV_2/Ni$ -based powders have greater capacities (about 2.2 times) than the amorphous parent alloy powders. Generally, the electrochemical properties are closely linked to the size and crystallographic perfection of the constituent grains, which in turn are a function of the processing or grain refinement method used to prepare the hydrogen storage alloys.

### 3.3 LaNi<sub>5</sub>-type alloys

The properties of hydrogen host  $LaNi_5$  materials can be modified substantially by alloying. It was found that the substitution of Ni in  $LaNi_5$  by small amounts of Al, Mn, Si, Zn, Cr, Fe, Cu or Co altered the hydrogen storage capacity, the stability of the hydride phase and the corrosion resistance [7]. Generally, in the transition metal sublattice of  $LaNi_5$ -type compounds, substitution by Mn, Al and Co has been found to offer the best compromise between high hydrogen capacity and good resistance to corrosion [8]. During the MA process originally sharp diffraction lines of La and Ni gradually become broader and their intensity decreases with milling time. The powder mixture milled for more than 30 h has transformed completely to the amorphous phase. Formation of the nanocrystalline alloy was achieved by annealing of the

amorphous material in high purity argon atmosphere at 973 K for 0.5 h (Fig. 1c). According to AFM studies, the average size of amorphous La-Ni powders was of order of 25 nm.

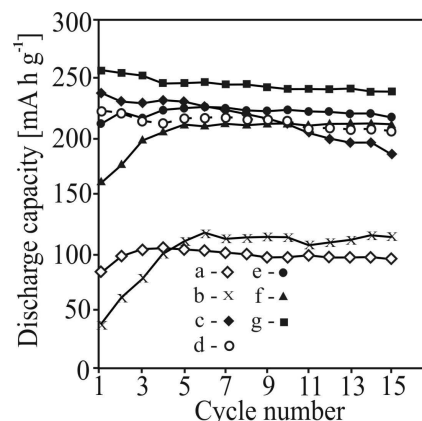


Fig. 4. Discharge capacities as a function of cycle number of  $LaNi_5$ -type negative electrodes made from nanocrystalline powders prepared by MA followed by annealing: a)  $LaNi_5$ , b)  $LaNi_4Co$ , c)  $LaNi_4Mn$ , d)  $LaNi_4Al$ , e)  $LaNi_{3.75}CoMn_{0.25}$ , f)  $LaNi_{3.75}CoAl_{0.25}$ , g)  $LaNi_{3.75}Mn_{0.75}Al_{0.25}Co_{0.25}$  (solution, 6 M KOH;  $T=293K$ ). The charge conditions were  $40 \text{ mA g}^{-1}$ . The cut-off potential vs.  $Hg/HgO/6 \text{ M KOH}$  was  $-0.7 \text{ V}$ .

The discharge capacity of an electrode prepared by application of nanocrystalline  $LaNi_5$  alloy powder is low (Fig. 4). It was found that the substitution of Ni by Al or Mn in  $La(Ni,M)_5$  alloy leads to an increase in discharge capacity. The  $LaNi_4Mn$  electrode, mechanically alloyed and annealed, displayed the maximum capacity at the 1<sup>st</sup> cycle but discharge capacity degraded strongly with cycling. On the other hand, alloying elements such as Al, Mn and Co substituting nickel greatly improved the cycle life of  $LaNi_5$ -type material (Fig. 4). With the increase of cobalt content in  $LaNi_{4-x}Mn_{0.75}Al_{0.25}Co_x$ , the material shows an increase in discharge capacity which passes through a wide maximum for  $x=0.25$ . In nanocrystalline  $LaNi_{3.75}Mn_{0.75}Al_{0.25}Co_{0.25}$  discharge capacities up to  $258 \text{ mA h g}^{-1}$  (at  $40 \text{ mA g}^{-1}$  discharge current) was measured, which compares with results reported by Iwakura et al. for polycrystalline  $MmNi_{4-x}Mn_{0.75}Al_{0.25}Co_x$  alloys (Mm-mishmetal) [13].

Recently the cleanliness of the surface of polycrystalline and nanocrystalline  $LaNi_5$ -type alloys was studied by X-ray photoelectron spectroscopy (XPS) and Auger electron spectroscopy (AES) [14]. Results showed that the level of oxygen impurities trapped in the mechanically alloyed powder during the processing is practically the same as in the arc-melted samples. The substitution of Ni by Al in  $LaNi_5$  leads to significant modifications of the electronic structure of the polycrystalline sample. Furthermore, the XPS valence band of the MA nanocrystalline  $LaNi_4Al_1$  alloy is considerable broader compared to that measured for the polycrystalline sample. The strong modifications of the

electronic structure and the significant surface segregation of lanthanum atoms in the MA nanocrystalline LaNi<sub>5</sub>-type alloys could significantly influence its hydrogenation properties.

### 3.4 Mg<sub>2</sub>Ni-type alloys

The magnesium-nickel phase diagram shows two compounds Mg<sub>2</sub>Ni and MgNi<sub>2</sub>. The first one reacts with hydrogen slowly at room temperature to form the ternary hydride Mg<sub>2</sub>NiH<sub>4</sub>. At higher temperatures at pressure (e.g. 473 K, 1.4 MPa), the reaction is rapid enough for useful absorption-desorption reactions to occur.

Mechanical alloying is one of the approaches to produce Mg-Ni alloys which have been highly expected to be used as hydrogen storage materials. Ling et al. [15] pointed out that HEBM which gives rise to the creation of fresh surfaces and cracks is highly effective for the kinetic improvement in initial hydriding properties.

In this work, the nanocrystalline Mg<sub>2</sub>Ni-type alloys were prepared by mechanical alloying followed by annealing. The powder mixture milled for more than 90 h has transformed completely to the amorphous phase, without formation of another phase. Formation of the nanocrystalline alloy was achieved by annealing of the amorphous material in high purity argon atmosphere at 723 K for 0.5 h. All diffraction peaks were assigned to those of the hexagonal crystal structure with cell parameters  $a = 0.5216$  nm,  $c = 1.3246$  nm (Fig. 1d). According to AFM studies, the average size of amorphous Mg-Ni powders was of the order of 30 nm.

At room temperature, the nanocrystalline Mg<sub>2</sub>Ni alloy absorbs hydrogen, but almost does not desorb it. At temperatures above 523 K the kinetic of the absorption-desorption process improves considerably and for nanocrystalline Mg<sub>2</sub>Ni alloy the reaction with hydrogen is reversible. The hydrogen content in this material at 573 K is 3.25 wt%. Upon hydrogenation, Mg<sub>2</sub>Ni transforms into the hydride Mg<sub>2</sub>NiH<sub>x</sub> phase. It is important to note, that between 518-483 K the hydride Mg<sub>2</sub>NiH<sub>x</sub> phase transforms from a high temperature cubic structure to a low temperature monoclinic phase. When hydrogen is absorbed by Mg<sub>2</sub>Ni beyond 0.3 H per formula unit, the system undergoes a structural rearrangement to the stoichiometric complex Mg<sub>2</sub>NiH<sub>x</sub> hydride, with an accompanying 32% increase in volume. The electrochemical properties of the alloy are improved after substitution of some amounts of magnesium by manganese. The results show that the maximum absorption capacity reaches 3.25 wt% for pure nanocrystalline Mg<sub>2</sub>Ni alloy. This is lower than the polycrystalline Mg<sub>2</sub>Ni alloy (3.6 wt% [8]) due to a significant amount of strain, chemical disorder and defects introduced into the material during the mechanical alloying process [6]. At the same time, increasing manganese substitution causes the unit cell to decrease. The concentration of hydrogen in produced nanocrystalline Mg<sub>2</sub>Ni alloys strongly decreases with

increasing Mn contents. The hydrogen content at 573 K in nanocrystalline Mg<sub>1.5</sub>Mn<sub>0.5</sub>NiH was only 0.65 wt%.

The Mg<sub>2</sub>Ni electrode, mechanically alloyed and annealed, displayed the maximum discharge capacity (100 mA h g<sup>-1</sup>) at the 1<sup>st</sup> cycle but degraded strongly with cycling. The poor cyclic behaviour of Mg<sub>2</sub>Ni electrodes is attributed to the formation of Mg(OH)<sub>2</sub> on the electrodes, which has been considered to arise from the charge-discharge cycles [16]. To avoid the surface oxidation, we have examined the effect of magnesium substitution by Mn or Al in Mg<sub>2</sub>Ni-type material. This alloying greatly improved the discharge capacities. In nanocrystalline Mg<sub>1.5</sub>Mn<sub>0.5</sub>Ni and Mg<sub>1.5</sub>Al<sub>0.5</sub>Ni alloys discharge capacities up to 241 mA h g<sup>-1</sup> and 175 mA h g<sup>-1</sup> were measured, respectively [9].

The surface chemical composition of nanocrystalline Mg<sub>2</sub>Ni-type alloy studied by X-ray photoelectron spectroscopy (XPS) showed the strong surface segregation under UHV conditions of Mg atoms in the MA nanocrystalline Mg<sub>2</sub>Ni alloy. This phenomenon could considerably influence the hydrogenation process in such a type of materials, as well.

### 3.5 Composite-type nanomaterials

A new class of electrode materials, composite hydride materials, is proposed for anodes in hydride based rechargeable batteries [17]. These materials were synthesized by mechanical mixing of two components: a major component having good hydrogen storage properties and a minor component used as surface activator. The major component was selected among conventional hydride electrode materials; alloys of the TiFe-, ZrV<sub>2</sub>-, LaNi<sub>5</sub>- and Mg<sub>2</sub>Ni-type type. The minor component was usually nickel or graphite. Till now, the composite hydride electrodes using Ni as minor component have shown the following advantages: almost a complete elimination of the need for initial activation, an enhancement of the discharge capacity, a considerable improvement in the stability to charge/discharge at high rates, an increase in the charging efficiency, a higher resistance to surface degradation during repeated charge/discharge.

In order to improve the electrochemical properties of the studied so far nanocrystalline electrode materials, the ball-milling technique was applied to the TiFe- and Mg<sub>2</sub>Ni-type alloys using the nickel and graphite elements as a surface modifiers [18]. The TiFe<sub>0.25</sub>Ni<sub>0.75</sub>/M- and Mg<sub>1.5</sub>Mn<sub>0.5</sub>Ni/M-type composite materials, where M=10 wt% Ni or C, were produced by ball-milling for 1 h and 30 min, respectively. Ball-milling with nickel or graphite of TiFe<sub>0.25</sub>Ni<sub>0.75</sub>- and Mg<sub>1.5</sub>Mn<sub>0.5</sub>Ni-type materials is sufficient to considerably broaden the diffraction peaks of TiFe<sub>0.25</sub>Ni<sub>0.75</sub> and Mg<sub>1.5</sub>Mn<sub>0.5</sub>Ni. Additionally, milling with graphite is responsible for a sizeable reduction of the crystallite sizes of TiFe<sub>0.25</sub>Ni<sub>0.75</sub>/C and Mg<sub>1.5</sub>Mn<sub>0.5</sub>Ni/C from 30 nm to 20 nm.

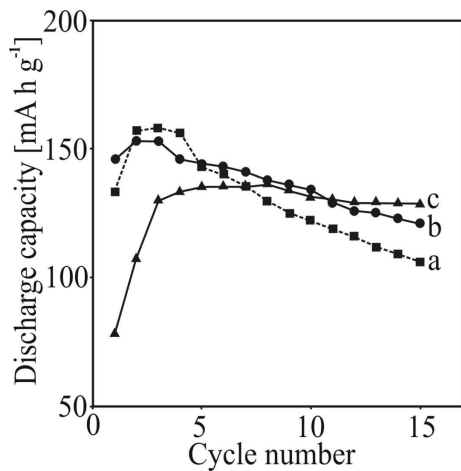


Fig. 5. The discharge capacity as a function of cycle number for MA and annealed  $\text{TiFe}_{0.25}\text{Ni}_{0.75}$  (a) as well as  $\text{TiFe}_{0.25}\text{Ni}_{0.75}/\text{Ni}$  (b) and  $\text{TiFe}_{0.25}\text{Ni}_{0.75}/\text{C}$  (c) composite electrodes (solution, 6 M KOH; temperature, 293 K).

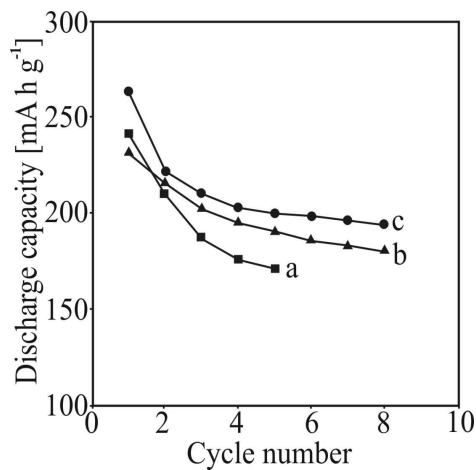


Fig. 6. The discharge capacity as a function of cycle number for MA and annealed  $\text{Mg}_{1.5}\text{Mn}_{0.5}\text{Ni}$  (a) as well as  $\text{Mg}_{1.5}\text{Mn}_{0.5}\text{Ni}/\text{Ni}$  (b) and  $\text{Mg}_{1.5}\text{Mn}_{0.5}\text{Ni}/\text{C}$  (c) composite electrodes (solution, 6 M KOH; temperature, 293 K).

When coated with nickel, the discharge capacities of nanocrystalline  $\text{TiFe}_{0.25}\text{Ni}_{0.75}$  and  $\text{Mg}_{1.5}\text{Mn}_{0.5}\text{Ni}$  powders were increased (Figs. 5 and 6). The elemental nickel was distributed on the surface of ball milled alloy particles homogeneously and role of these particles is to catalyse the dissociation of molecular hydrogen on the surface of studied alloy. Mechanical coating with nickel or graphite effectively reduced the degradation rate of the studied electrode materials. Compared to that of the uncoated powders, the degradation of the coated was suppressed. Recently, Raman and XPS investigations indicated the interaction of graphite with MgNi alloy occurred at the Mg part in the alloy [19]. Graphite inhibits the formation of new oxide layer on the surface of materials once the native oxide layer is broken during the ball-milling process.

#### 4. Closed cells

The cyclic behavior of the some nanocrystalline TiFe-type alloy anodes was examined in a sealed HB 116/054 cell (according to the International standard IEC no. 61808, related to the hydride button rechargeable single cell) [20]. The mass of the active material was 0.33 g. To prepare MH negative electrodes, alloy powders were mixed with addition of 5 wt.% tetracarbonylnickel. Then this mixture was pressed into the form tablets which were placed in a small basket made of nickel nets (as the current collector). The diameter of each tested button cells was 6.6 mm and a thickness of 2.25 mm, respectively. The sealed Ni-MH cell was constructed by the pressing negative and positive electrode, polyamide separator and KOH ( $\rho = 1.20 \cdot 10^{-3} \text{ kg m}^{-3}$ ) as electrolyte solution. The battery with electrode fabricated from nanocrystalline materials was charged at current density of  $i = 3 \text{ mA g}^{-1}$  for 15 h and after 1 h pause discharged at current density of  $i = 7 \text{ mA g}^{-1}$  down to 1.0 V. All electrochemical measurements were performed at  $293 \pm 1 \text{ K}$ .

Fig. 7 shows the discharge capacities of sealed button cells with electrodes prepared from nanocrystalline  $\text{TiFe}_{0.25}\text{Ni}_{0.75}$  and TiNi alloys as a function of discharge cycle number. The electrode and sealed battery using the nanocrystalline  $\text{TiFe}_{0.25}\text{Ni}_{0.75}$  alloy show better characteristics than that using the nanocrystalline TiNi alloy. The results show that the sealed battery using the nanocrystalline  $\text{TiFe}_{0.25}\text{Ni}_{0.75}$  alloy has the capacity of the polycrystalline  $(\text{Zr}_{0.35}\text{Ti}_{0.65})(\text{V}_{0.93}\text{Cr}_{0.28}\text{Fe}_{0.19}\text{Ni}_{1.0})$  one.

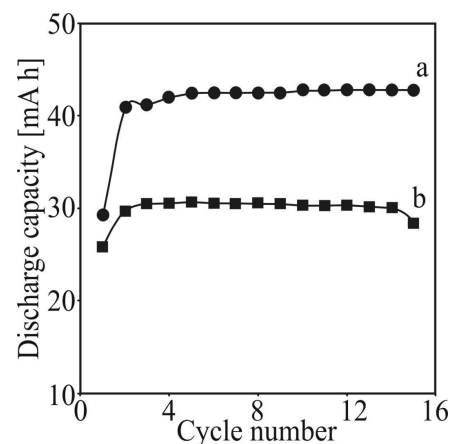


Fig. 7. Durability of the sealed button cells with negative electrodes made from nanocrystalline: a)  $\text{TiFe}_{0.25}\text{Ni}_{0.75}$  and b) TiNi alloys (the mass of the active material was 0.33 g).

Independently, it was found that the discharge capacities of sealed button cells with electrodes prepared from the nanocrystalline  $\text{La}(\text{Ni}, \text{Mn}, \text{Al}, \text{Co})_5$  powders had a slightly higher discharge capacities, compared with negative electrodes prepared from polycrystalline powders.

## 5. Conclusion

In conclusion, nanocrystalline TiFe-, ZrV<sub>2</sub>-, LaNi<sub>5</sub>- and Mg<sub>2</sub>Ni-type alloys synthesized by mechanical alloying can reversibly store hydrogen to form hydride and release hydrogen electrochemically. The hydrogen storage properties of nanocrystalline ZrV<sub>2</sub>- and LaNi<sub>5</sub>-type powders prepared by mechanical alloying and annealing show no big difference with those of melt casting (polycrystalline) alloys. On the other hand, the nanocrystalline TiFe- and Mg<sub>2</sub>Ni-type hydrides show substantially enhanced absorption characteristics superior to those of the conventionally prepared materials. The properties of nanocrystalline electrode were attributed to the structural characteristics of the compound caused by mechanical alloying. Mechanical alloying is a suitable procedure for obtaining nanocrystalline hydrogen storage materials with high capacities and better hydrogen sorption properties. At present, the Ni-MH battery is a key component for advanced information and telecommunication systems. The input materials for this high-tech battery would be nanocrystalline hydrogen storage alloys.

## Acknowledgements

The financial support of the Polish National Committee for Scientific Research under the contracts No: KBN-7 T08D 015 12 (1997-2000), PBZ/KBN-013/T08/02 (2000-2003), KBN-8 T10A 001 20 (2001-2004) and KBN-3T10A 033 29 (2005-2008) is gratefully acknowledged.

## References

- [1] C. Suryanarayana, *Progr. Mater. Sc.* **46**, 1 (2001).
- [2] A. Anani, A. Visintin, K. Petrov, S. Srinivasan, J. J. Reilly, J.R. Johnson, R. B. Schwarz, P. B. Desch, *J. Power Sources* **47**, 261 (1994).
- [3] M. Jurczyk, *Current Topics in Electrochem.* **9**, 105 (2003).
- [4] M. Jurczyk, L. Smardz, M. Makowiecka, E. Jankowska, K. Smardz, *J. Phys. Chem. Sol.* **65**, 545 (2004).
- [5] M. Jurczyk, L. Smardz, A. Szajek, *Mat. Sc. Eng. B* **108**, 67 (2004).
- [6] L. Zaluski, A. Zaluska, J. O. Ström-Olsen, *J. Alloys Comp.* **253–254**, 70 (1997).
- [7] K. H. J. Buschow, P. C. P. Bouten, A. R. Miedema, *Rep. Prog. Phys.* **45**, 937 (1982).
- [8] T. Sakai, M. Matsuoka, C. Iwakura, Chapter 142 in: K. A. Gschneider Jr., L. Eyring (Eds), *Handbook on the Physics and Chemistry of Rare Earth*, Vol. 21: Elsevier Science B.V., (1995).
- [9] A. Gasiorowski, W. Iwasieczko, D. Skoryna, H. Drulis, M. Jurczyk, *J. Alloys Comp.* **364**, 283 (2004).
- [10] M. Jurczyk, E. Jankowska, M. Nowak, I. Wieczorek, *J. Alloys Comp.* **354**, L1 (2003).
- [11] M. Jurczyk, E. Jankowska, M. Nowak, J. Jakubowicz, *J. Alloys Comp.* **336**, 265 (2002).
- [12] M. Jurczyk, W. Rajewski, W. Majchrzycki, G. Wojcik, *J. Alloys Comp.* **274**, 299 (1998).
- [13] C. Iwakura, K. Fukuda, H. Senoh, H. Inoue, M. Matsuoka, Y. Yamamoto, *Electrochim. Acta* **43**, 2041 (1998).
- [14] M. Jurczyk, K. Smardz, W. Rajewski, L. Smardz, *Mater. Sc. Eng.* **A303**, 70 (2001).
- [15] G. Ling, S. Boily, J. Huot, A. Van Neste, R. Schultz, *J. Alloys Comp.* **268**, 302 (1998).
- [16] D. Mu, Y. Hatano, T. Abe, K. Watanabe, *J. Alloys Comp.* **334**, 232 (2002).
- [17] J. Chen, D. H. Bradhurst, S. X. Don, H. K. Liu, *J. Alloys Comp.* **280**, 290 (1998).
- [18] M. Jurczyk, *J. Mater. Sc.* **39**, 5271 (2004).
- [19] C. Iwakura, H. Inoue, S. G. Zhang, S. Nohara, *J. Alloys Comp.* **293–295**, 653 (1999).
- [20] E. Jankowska, M. Jurczyk, *J. Alloys Comp.* **372**, L9 (2004).

Corresponding author: jurczyk@sol.put.poznan.pl